Organic LETTERS

Letter

Cite This: Org. Lett. 2018, 20, 7020–7023

pubs.acs.org/OrgLett

Hierarchical Self-Assembly of a Water-Soluble Organoplatinum(II) Metallacycle into Well-Defined Nanostructures

Sougata Datta,*[,†] Manik Lal Saha,*[,†] Nabajit Lahiri,[†] Guocan Yu,[‡] Janis Louie,*[,†] and Peter J. Stang*[,†]

[†]Department of Chemistry, University of Utah, 315 South 1400 East, Room 2020, Salt Lake City, Utah 84112, United States

[‡]State Key Laboratory of Chemical Engineering, Center for Chemistry of High-Performance & Novel Materials, Department of Chemistry, Zhejiang University, Hangzhou 310027, P. R. China

Supporting Information

ABSTRACT: A water-soluble metallosupramolecular hexagon containing pendant methyl viologen (MV) and trimethylammonium units at the vertices has been synthesized via an organoplatinum(II) ← pyridyl coordination-driven self-assembly reaction. The MV units of the metallacycle were further utilized in the formation of a heteroternary complex with cucurbit[8]uril and a galactose-functionalized naphthalene derivative, yielding a metallacycle-cored carbohydrate cluster that was subsequently ordered into nanospheres and tapes, depending upon the concentration.

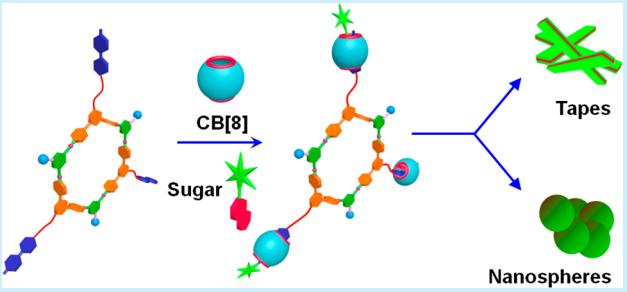

Carbohydrates play crucial roles in various biological processes: bacterial or viral infection, fertilization, immune response, tumor-cell metastasis, etc., via enabling specific recognition interactions between a glyco cluster and a protein.[1] Given these intricate functions, various synthetic carbohydrate-containing functional scaffolds including glycoproteins, polymers, dendrimers, carbon nanomaterials, calixarenes, pillararenes, etc. have been prepared via covalent synthesis.[2] In contrast to the tedious covalent approach, supramolecular chemistry, in particular coordination-driven self-assembly via metal−ligand bonding, is a viable strategy, whereby a fast and efficient one-pot synthesis of diverse supramolecular coordination complexes (SCCs) can be accomplished.[3] Due to their well-defined shapes and sizes, SCCs are excellent platforms to install functional units either on the periphery or at the vertices, resulting in functional systems, such as sensors and catalysts, etc.[4] Functionalized SCCs are currently synthesized from appropriate prefunctionalized precursors whose preparations involve some additional covalent synthesis of organic ligands or metal acceptors.[5] Recently, hierarchical self-assembly techniques have emerged as a new strategy, wherein multiple orthogonal interactions between molecular precursors can produce functional structures while keeping the synthetic steps at a minimum. For example, a precise unification of coordination-driven self-assembly with crown ether based host−guest interactions leads to the formation of robust metallacycle-cored supramolecular polymer gels in organic solvents.[6] The hierarchical approach is, however, much less explored in aqueous medium due to the intrinsic hydrophobicity of SCCs, restricting the implementation of biologically relevant functionalities, such as sugars, into the SCC platforms.[7]

Cucurbit[*n*]urils (CB[*n*], *n* = 5−8, 10, 14) are a family of pumpkin-shaped macrocyclic cavitands, having repetitive glycoluril units interconnected by methylene groups.[8] Among the CB[*n*] homologues, CB[8] is capable of accommodating two identical or different small guest molecules in its cavity in water.[9] For example, amino acids and peptides form noncovalent homodimers (1:2) with CB[8], while heterodimerizations (1:1:1) were observed with dicationic species such as methyl viologen (MV) and 2,7-dimethyldiazaphenanthrenium and electron-rich aromatic molecules such as naphthalene, indole, etc. ($K_a \geq 10^{11}$ M^{-2}).[10] This unique property of CB[8] has been utilized for the preparation of microcapsules for on-demand release, tunable emission, supramolecular polymerization, catalysis, protein dimerization, enzymatic activity, etc.[11]

Herein, we combine the organoplatinum(II) ← pyridyl coordination-driven self-assembly with CB[8]-mediated host−guest interactions to report the synthesis of a metallacycle-cored carbohydrate cluster (Scheme 1) that subsequently formed various nanostructures, such as nanospheres and tapes, depending upon the concentration. In these hierarchical nanostructures, the metal−ligand coordination provides the first level of organization, while host−guest interaction and hydrogen bonding derived from CB[8] and sugar units enable the higher-order organizations. The approach described herein provides a facile strategy to prepare carbohydrate functional materials that can be useful for biomedical research. As shown in Scheme 1, the synthesis of hexagon **1** requires a 120° dipyridyl donor **2**·2PF_6^- and a 120° organoplatinum acceptor

Received: September 12, 2018
Published: October 29, 2018

DOI: 10.1021/acs.orglett.8b02925
Org. Lett. 2018, 20, 7020–7023

Scheme 1. Preparation of Discrete Metallacyclic Hexagon 1 and Cartoon Representation of the Formation of Heteroternary Host–Guest Complex 5 from 1, CB[8], and NG

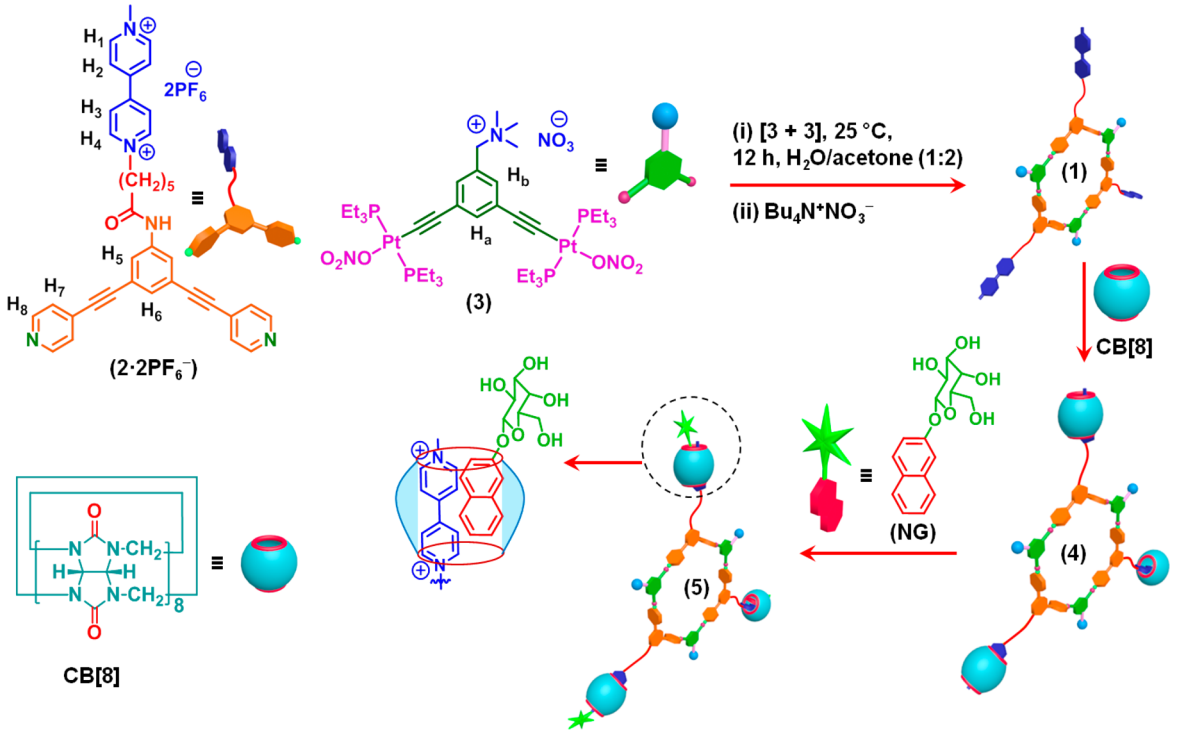

3. The former was prepared by a 1-ethyl-3-(3-(dimethylamino)propyl)carbodiimide hydrochloride (EDC·HCl) mediated amidation reaction between **6**[12] and **7**[13] in 70% yield (Scheme 2A). While the multistep synthesis of the new metal acceptor **3** commenced with a nucleophilic substitution reaction that transformed **8**[14] into **9** (Scheme 2B), a palladium-catalyzed Sonogashira reaction of **9** with (trimethylsilyl)acetylene delivered a trimethylsilyl-protected acetylene derivative that provided precursor **10** after hydrolysis (65% isolated yield). Compound **10** was then reacted with 4 equiv of *trans*-$PtI_2(PEt_3)_2$ to prepare **11**, which upon reaction with methyl iodide, followed by anion metathesis with $AgNO_3$, resulted in **3** in good yield. Subsequently, the self-assembled [3 + 3] hexagon **1** was obtained by stirring a mixture of MV-functionalized 120° dipyridyl donor, **2·2PF$_6^-$**, and 120° organoplatinum(II) acceptor **3** in a 1:1 stoichiometry in H_2O/acetone (1:2 v/v) at room temperature for 12 h, followed by anion exchange using tetrabutylammonium nitrate (Scheme 1). The resulting hexagon **1** is water soluble, although the corresponding precursors **2·2PF$_6^-$** and **3** are water insoluble.

In the ^{1}H NMR spectrum of **1** (Figure 1A), the pyridyl protons H_8 and H_7 of **2** showed downfield shifts ($\Delta\delta[H_8]$ = 0.24 ppm; $\Delta\delta[H_7]$ = 0.28 ppm) with reference to those of the free **2·2NO$_3^-$** (Figure 1B) due to the coordination of the pyridyl N atoms to the Pt centers. Likewise, the ^{31}P{^{1}H} NMR spectrum of **1** revealed a single sharp singlet at ∼16.97 ppm with concomitant ^{195}Pt satellites (J_{Pt-P} = 2303 Hz), consistent with a single phosphorus environment (Figure 1D). This signal shifted upfield by 4.49 ppm relative to that of acceptor **3** (Figure 1E). The decrease in the coupling of ^{195}Pt satellites (ca. ΔJ = 99 Hz) in **1** relative to that of **3** is consistent with the electron backdonation from the platinum centers.

The formation of **1** was further supported by electrospray ionization time-of-flight mass spectrometry (ESI-TOF-MS). In the mass spectrum of **1**, two peaks were identified that support the formation of a [3 + 3] assembly: m/z = 1387.51 Da for $[M - 4ONO_2]^{4+}$ and m/z = 1097.61 Da for $[M - 5ONO_2]^{5+}$. Both peaks were isotopically resolved and matched well with their calculated theoretical distributions (Figure S26, Supporting Information (SI)). All attempts to grow X-ray single crystals of **1** have thus far proven unsuccessful, likely due to the flexibility of the alkyl chains. PM6 semiempirical computations of **1** (Figure S27, SI) featured a planar hexagonal ring at the core with an internal diameter of 2.80 nm. The ring is surrounded by three MV units and three trimethylammonium (TMA) groups alternatively at the vertices. The host–guest complexation between **1** and CB[8] was studied by ^{1}H NMR experiments in D_2O (Figure S29, SI). The signal at 9.05 and 9.15 ppm of **1** was assigned to the H_1 and H_4 protons of the MV units (Figures S28 and S29A, SI). They shifted upfield in **4**=[**1**·(CB[8])$_3$], merged with the peak of pyridyl H_8 protons, and appeared as a broad peak at 8.8 ppm due to host–guest complexation (Figure S29B, SI). Upon subsequent heteroternary host–guest complexation with 3 equiv of **NG**, this peak of **4** split into two sets and appeared at 8.4 and 8.8 ppm, where the former was assigned to the H_1 and H_4 protons of the MV units and the latter was assigned to the pyridyl H_8 protons. (Figure S29C, SI). At the same time, the **NG** protons appeared in the range of 7.4–8.0 ppm and experienced a significant upfield shift in **5**=[**4**·(**NG**)$_3$] (Figures S29C and D, SI). These upfield shifts in the ^{1}H NMR spectra are diagnostic for the heteroternary complexation.[15] The presence of galactose units does not interfere with such heteroternary complexation (Figure S30, Supporting Information).

The morphologies of the self-assembled aggregates of **1**, **4**, and **5** in water were examined using transmission electron

DOI: 10.1021/acs.orglett.8b02925
Org. Lett. 2018, 20, 7020–7023

Scheme 2. Synthesis of (A) MV-Functionalized Dipyridyl Donor $2{\cdot}2PF_6^-$ and (B) TMA-Pendent Organoplatinum(II) Acceptor 3[a]

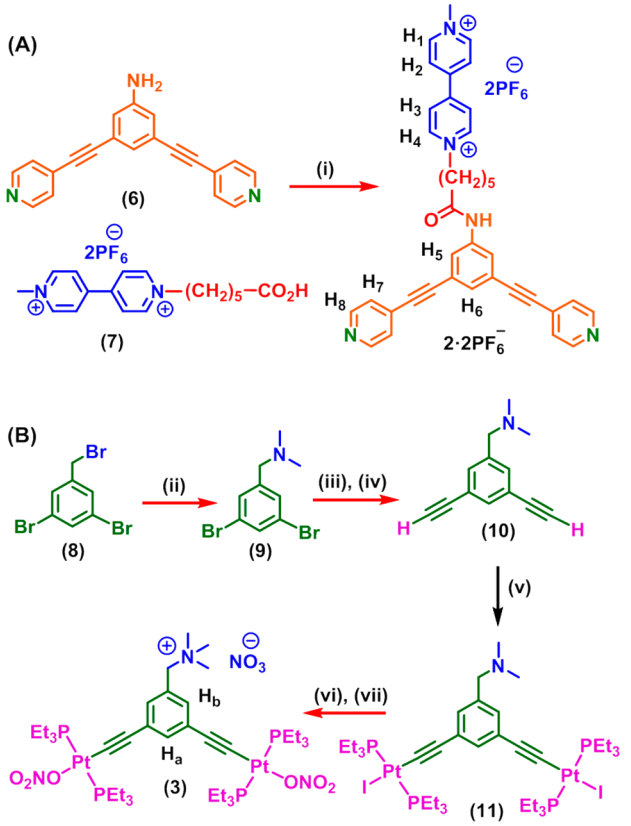

[a]Conditions: (i) EDC·HCl, DMAP, DMF, 48 h, room temperature, 70%; (ii) aq. Me_2NH, K_2CO_3, THF, 6 h, 60 °C (90%); (iii) and (iv) (trimethylsilyl)acetylene, $Pd(PPh_3)_4$, CuI, Et_3N, THF, 24 h, 60 °C; KOH, methanol, 24 h, room temperature, (95%); (v) *trans*-$PtI_2(PEt_3)_2$, CuI, Et_2NH, toluene, room temperature, 16 h (57%); (vi) and (vii) MeI, CH_2Cl_2, reflux, 24 h; $AgNO_3$, CH_2Cl_2, room temperature, 12 h (90%).

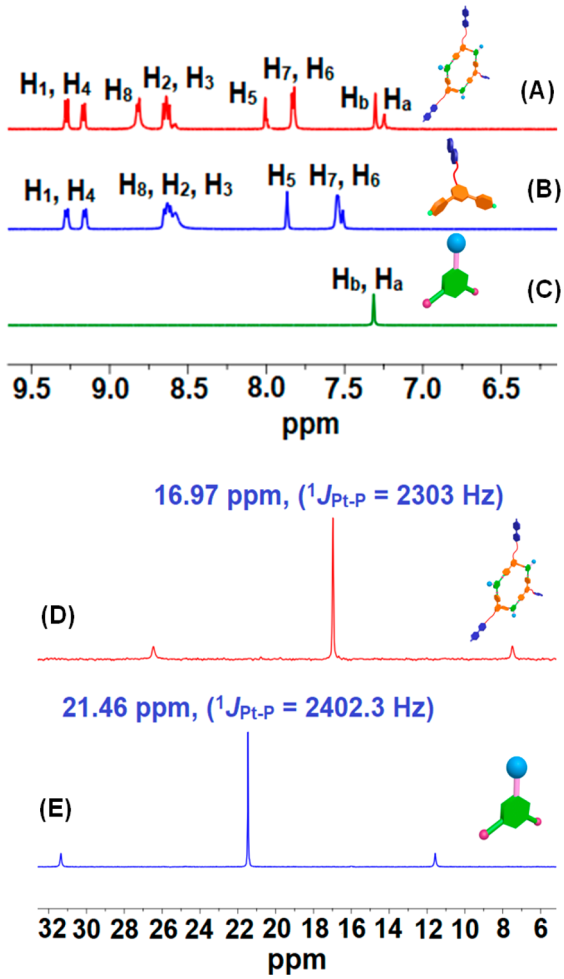

Figure 1. (A–C) Partial ^1H and (D, E) ^{31}P NMR spectra (CD_3OD, 25 °C) of (A,D) hexagonal metallacycle **1**, (B) donor $2{\cdot}2NO_3^-$, and (C,E) acceptor **3**.

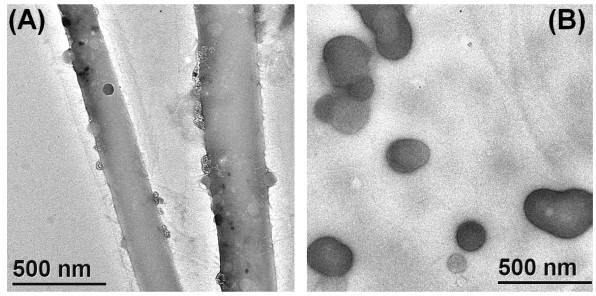

Figure 2. TEM images of the aggregates obtained from the aqueous solutions of **5** after standing for 1 week at concentrations of (A) 17 and (B) 3.4 μM, respectively.

microscopy (TEM). Spherical nanoparticles with a diameter of ca. 14 nm were formed by **1** at a concentration of 17 μM (Figure S31A, SI). A dynamic light scattering (DLS) experiment performed with a 17 μM aqueous solution of **1** showed a narrow size distribution (Figure S33A, SI). The average hydrodynamic diameter (D_h) of **1** was observed to be 15 nm in good accordance with the TEM results. The host–guest complex **4** formed globular aggregates with an average size of 100 nm (Figures S31B and S33B, SI). The heteroternary complex **5** showed tape-like morphology with widths of about 30–200 nm at a concentration of 17 μM (Figure S31C, SI). However, it is evident from the TEM image that the tape-like structure is not well developed (Figure S31C, SI). Nicely formed tapes with widths of about 200–300 nm were obtained after keeping the aqueous solution of **5** (17 μM) at room temperature for 1 week (Figure 2A).

At a concentration of 3.4 μM, **5** exhibited lump-like aggregates (Figure S31D, SI) which transformed into nanospheres with diameters of 80–200 nm upon standing of the aqueous solution at room temperature for 1 week (Figure 2B). DLS data revealed the average size of the nanospheres to be ca. 140 nm (Figure S33C, SI), which is consistent with the TEM result (Figure 2B). Likewise, Yan et al. observed morphological transition from sphere-to-fiber/ribbon upon increasing the concentration of organoplatinum rhomboids having hydrophilic PEG groups at the vertices.[16] Additionally, STEM-EDS (STEM, scanning transmission electron microscopy; EDS, energy-dispersive spectroscopy) spectra of the above samples further confirmed the presence of carbon, nitrogen, oxygen, phosphorus, and platinum in the aggregates (Figure S32, SI). We further investigated the effect of adding an excess of 2-naphthol to **5**. Lump-like aggregates of **5** were still observed after addition of 3 equiv (with respect to **1**) of 2-naphthol

DOI: 10.1021/acs.orglett.8b02925
Org. Lett. 2018, 20, 7020–7023

(Figure S31G, SI), whereas upon addition of 9 equiv of 2-naphthol the lumps were disassembled (Figure S31I, SI).

In summary, a multicationic organoplatinum(II) hexagon **1** was prepared by means of coordination-driven self-assembly. The cationic groups at the periphery of **1** overcome its hydrophobicity attributed to the hexagonal aromatic core and triethylphosphine groups and render it water-soluble. The MV units of **1** form a noncovalent host−guest complex with CB[8] that can further undergo heteroternary complexation with **NG** forming **5**. The host−guest complexation processes were accompanied by morphological transformations that were studied by ^{1}H NMR spectroscopy, TEM, and DLS experiments. The heteroternary complex **5** resulted in a tape-like morphology after its aqueous solution was kept at room temperature for 1 week. The galactose units at the surface of the tape-like structures may endow them with interesting biofunction. Exploration of biological applications of these nanostructures is underway in our laboratory.

■ ASSOCIATED CONTENT

Supporting Information

The Supporting Information is available free of charge on the ACS Publications website at DOI: 10.1021/acs.orglett.8b02925.

Experimental details, NMR spectra, and other materials (PDF)

■ AUTHOR INFORMATION

Corresponding Authors

*E-mail: sougata.datta@utah.edu.
*E-mail: manik.saha@utah.edu.
*E-mail: louie@chem.utah.edu.
*E-mail: stang@chem.utah.edu.

ORCID

Manik Lal Saha: 0000-0003-2242-3007
Janis Louie: 0000-0003-3569-1967
Peter J. Stang: 0000-0002-2307-0576

Notes

The authors declare no competing financial interest.

■ ACKNOWLEDGMENTS

P.J.S. and S.D., respectively, thank the NIH (R01-CA215157) and SERB Indo-U.S. Postdoctoral fellowship for financial support.

■ REFERENCES

(1) (a) Illescas, B. M.; Rojo, J.; Delgado, R.; Martín, N. *J. Am. Chem. Soc.* **2017**, *139*, 6018−6025. (b) Bhatia, S.; Camacho, L. C.; Haag, R. *J. Am. Chem. Soc.* **2016**, *138*, 8654−8666. (c) Sato, S.; Yoshimasa, Y.; Fujita, D.; Yagi-Utsumi, M.; Yamaguchi, T.; Kato, K.; Fujita, M. *Angew. Chem., Int. Ed.* **2015**, *54*, 8435−8439.

(2) (a) Liu, Y.; Zhang, Y.; Wang, Z.; Wang, J.; Wei, K.; Chen, G.; Jiang, M. *J. Am. Chem. Soc.* **2016**, *138*, 12387−12394. (b) Park, S.; Kim, G.-H.; Park, S.-H.; Pai, J.; Rathwell, D.; Park, J.-Y.; Kang, Y.-S.; Shin, I. *J. Am. Chem. Soc.* **2015**, *137*, 5961−5968. (c) Zhang, S.; Moussodia, R.-O.; Sun, H.-J.; Leowanawat, P.; Muncan, A.; Nusbaum, C.-D.; Chelling, K. M.; Heiney, P. A.; Klein, M. L.; André, S.; Roy, R.; Gabius, H.-J.; Percec, V. *Angew. Chem., Int. Ed.* **2014**, *53*, 10899−10903. (d) Yu, G.; Ma, Y.; Han, C.; Yao, Y.; Tang, G.; Mao, Z.; Gao, C.; Huang, F. *J. Am. Chem. Soc.* **2013**, *135*, 10310−10313. (e) Pasparakis, G.; Cockayne, A.; Alexander, C. *J. Am. Chem. Soc.* **2007**, *129*, 11014−11015. (f) El-Boubbou, K.; Gruden, C.; Huang, X. *J. Am. Chem. Soc.* **2007**, *129*, 13392−13393. (g) Wang, H.; Gu, L.; Lin, Y.; Lu, F.; Meziani, M. J.; Luo, P. G.; Wang, W.; Cao, L.; Sun, Y.-P. *J. Am. Chem. Soc.* **2006**, *128*, 13364−13365.

(3) (a) Li, Z.; Yan, X.; Huang, F.; Sepehrpour, H.; Stang, P. J. *Org. Lett.* **2017**, *19*, 5728−5731. (b) Wang, S.; McGuirk, C. M.; Ross, M. B.; Wang, S.; Chen, P.; Xing, H.; Liu, Y.; Mirkin, C. A. *J. Am. Chem. Soc.* **2017**, *139*, 9827−9830. (c) Xie, T.-Z.; Wu, X.; Endres, K. J.; Guo, Z.; Lu, X.; Li, J.; Manandhar, E.; Ludlow, J. M., III.; Moorefield, C. N.; Saunders, J. M.; Wesdemiotis, C.; Newkome, G. R. *J. Am. Chem. Soc.* **2017**, *139*, 15652−15655. (d) Mosquera, J.; Szyszko, B.; Ho, S. K. Y.; Nitschke, J. R. *Nat. Commun.* **2017**, *8*, 14882. (e) Cook, T. R.; Stang, P. J. *Chem. Rev.* **2015**, *115*, 7001−7045.

(4) (a) Sinha, I.; Mukherjee, P. S. *Inorg. Chem.* **2018**, *57*, 4205−4221. (b) Chan, A. K.-W.; Ng, M.; Wong, Y.-C.; Chan, M.-Y.; Wong, W.-T.; Yam, V. W.-W. *J. Am. Chem. Soc.* **2017**, *139*, 10750−10761. (c) Bloch, W. M.; Holstein, J. J.; Hiller, W.; Clever, G. H. *Angew. Chem., Int. Ed.* **2017**, *56*, 8285−8289. (d) Saha, M. L.; Yan, X.; Stang, P. J. *Acc. Chem. Res.* **2016**, *49*, 2527−2539. (e) Sun, B.; Wang, M.; Lou, Z.; Huang, M.; Xu, C.; Li, X.; Chen, L.-J.; Yu, Y.; Davis, G. L.; Xu, B.; Yang, H.-B.; Li, X.-P. *J. Am. Chem. Soc.* **2015**, *137*, 1556−1564. (f) Kishi, N.; Akita, M.; Kamiya, M.; Hayashi, S.; Hsu, H.-F.; Yoshizawa, M. *J. Am. Chem. Soc.* **2013**, *135*, 12976−12979.

(5) Zhou, F.; Li, S.; Cook, T. R.; He, Z.; Stang, P. J. *Organometallics* **2014**, *33*, 7019−7022.

(6) Yan, X.; Cook, T. R.; Pollock, J. B.; Wei, P.; Zhang, Y.; Yu, Y.; Huang, F.; Stang, P. J. *J. Am. Chem. Soc.* **2014**, *136*, 4460−4463.

(7) (a) Datta, S.; Saha, M. L.; Stang, P. J. *Acc. Chem. Res.* **2018**, *51*, 2047−2063. (b) Wei, P.; Yan, X.; Huang, F. *Chem. Soc. Rev.* **2015**, *44*, 815−832.

(8) Murray, J.; Kim, K.; Ogoshi, T.; Yao, W.; Gibb, B. C. *Chem. Soc. Rev.* **2017**, *46*, 2479−2496.

(9) Assaf, K. I.; Nau, W. M. *Chem. Soc. Rev.* **2015**, *44*, 394−418.

(10) (a) Datta, S.; Misra, S. K.; Saha, M. L.; Lahiri, N.; Louie, J.; Pan, D.; Stang, P. J. *Proc. Natl. Acad. Sci. U. S. A.* **2018**, *115*, 8087−8092. (b) Barrow, S. J.; Kasera, S.; Rowland, M. J.; del Barrio, J.; Scherman, O. A. *Chem. Rev.* **2015**, *115*, 12320−12406.

(11) (a) Liu, J.; Lan, Y.; Yu, Z.; Tan, C. S. Y.; Parker, R. M.; Abell, C.; Scherman, O. A. *Acc. Chem. Res.* **2017**, *50*, 208−217. (b) Ni, X.-L.; Chen, S.; Yang, Y.; Tao, Z. *J. Am. Chem. Soc.* **2016**, *138*, 6177−6183. (c) Zheng, L.; Sonzini, S.; Ambarwati, M.; Rosta, E.; Scherman, O. A.; Herrmann, A. *Angew. Chem., Int. Ed.* **2015**, *54*, 13007−13011. (d) Huang, Z.; Yang, L.; Liu, Y.; Wang, Z.; Scherman, O. A.; Zhang, X. *Angew. Chem., Int. Ed.* **2014**, *53*, 5351−5355. (e) Zhang, K.-D.; Tian, J.; Hanifi, D.; Zhang, Y.; Sue, A. C.-H.; Zhou, T.-Y.; Zhang, L.; Zhao, X.; Liu, Y.; Li, Z.-T. *J. Am. Chem. Soc.* **2013**, *135*, 17913−17918. (f) Dang, D. T.; Nguyen, H. D.; Merkx, M.; Brunsveld, L. *Angew. Chem., Int. Ed.* **2013**, *52*, 2915−2919. (g) Reczek, J. J.; Kennedy, A. A.; Halbert, B. T.; Urbach, A. R. *J. Am. Chem. Soc.* **2009**, *131*, 2408−2415.

(12) Pollock, J. B.; Cook, T. R.; Stang, P. J. *J. Am. Chem. Soc.* **2012**, *134*, 10607−10620.

(13) Yamaguchi, H.; Harada, A. *Biomacromolecules* **2002**, *3*, 1163−1169.

(14) Gök, Y.; Noël, T.; Van der Eycken, J. *Tetrahedron: Asymmetry* **2010**, *21*, 2768−2774.

(15) (a) Samanta, S. K.; Moncelet, D.; Briken, V.; Isaacs, L. *J. Am. Chem. Soc.* **2016**, *138*, 14488−14496. (b) Kim, H.-J.; Heo, J.; Jeon, W. S.; Lee, E.; Kim, J.; Sakamoto, S.; Yamaguchi, K.; Kim, K. *Angew. Chem., Int. Ed.* **2001**, *40*, 1526−1529.

(16) Yan, X.; Li, S.; Cook, T. R.; Ji, X.; Yao, Y.; Pollock, J. B.; Shi, Y.; Yu, G.; Li, J.; Huang, F.; Stang, P. J. *J. Am. Chem. Soc.* **2013**, *135*, 14036−14039.

DOI: 10.1021/acs.orglett.8b02925
Org. Lett. 2018, 20, 7020−7023